

## ***In situ* x-ray diffraction study of the pressure-induced phase transformation in nanocrystalline CeO<sub>2</sub>**

Zhongwu Wang,<sup>1,\*</sup> S. K. Saxena,<sup>1</sup> V. Pischedda,<sup>1</sup> H. P. Liermann,<sup>1</sup> and C. S. Zha<sup>2</sup>

<sup>1</sup>*Center for the Study of Matter at Extreme Condition (CeSMEC), Florida International University, Miami, Florida 33199*

<sup>2</sup>*Cornell High Energy Synchrotron Source (CHESS), Wilson Laboratory, Cornell University, Ithaca, New York 14853*

(Received 20 February 2001; published 12 June 2001)

The x-ray-diffraction study of nanosized CeO<sub>2</sub> was carried to pressures of 38.6 GPa using an energy dispersive synchrotron-radiation technique in a diamond-anvil cell. At a pressure of 22.3 GPa, nano-CeO<sub>2</sub> starts to transform to an orthorhombic  $\alpha$ -PbCl<sub>2</sub> structure. This pressure is significantly lower than the transition pressure of 31 GPa for phase transformation in the bulk CeO<sub>2</sub>. The high-pressure phase is unquenchable and distorts to a hexagonal structure upon release of pressure to ambient conditions. The nanosized cubic fluorite phase has a bulk modulus ( $B_0$ ) of  $328 \pm 12$  GPa, much higher than that of the macrosized CeO<sub>2</sub> with a  $B_0$  of 230 GPa. There is a large volume decrease of 9.4% in phase transformation from the fluorite to  $\alpha$ -PbCl<sub>2</sub> structure. Such a phase transformation may occur via a large volume collapse and an unstable high-pressure phase causing a reduction of transition pressure in this type of nanomaterial.

DOI: 10.1103/PhysRevB.64.012102

PACS number(s): 62.50.+p, 81.40.Vw, 61.10.Nz

### I. INTRODUCTION

Pressure-induced phase transformations in fluorite-type compounds have been the subject of some recent studies.<sup>1</sup> Pressure-induced post-fluorite phases are of geophysical interest, and hence several fluorite-type dioxides have been subjected to high pressures up to 70 GPa and temperatures around 1000 °C, in a laser-heated diamond-anvil cell.<sup>2,3</sup> In materials that are quenched after high-pressure high-temperature treatment, phase transformations to denser structures have been reported.<sup>1-6</sup> Pressure Raman studies on the alkaline-earth difluorides have shown that they undergo a cubic-to-orthorhombic phase transformation at elevated pressure.<sup>1-3,6-8</sup> CeO<sub>2</sub> has the same type of structure as the dioxides and has been found to incorporate into the orthorhombic structure at pressures around 31 GPa at room temperature.<sup>7,8</sup>

There is now a considerable interest to investigate high-pressure behavior of nanosized materials due to their novel properties, which may differ from that of the macrosized materials.<sup>9-13</sup> Studies on nano-oxides indicate that the decrease of particle size significantly changes the compressibility and the transition pressure. Some of these oxides display lower transition pressure with a decrease in particle size.<sup>9,11,13</sup> Such findings are contrary to the general model for most nanomaterials, including sulfides and oxides, which exhibit higher transition pressures with a decrease in particle size.<sup>10,12</sup> Large volume collapse in this type of pressure-induced phase transformation is the explanation assigned to such observations.<sup>10</sup> However, to deepen our understanding of this new high-pressure phenomenon in the nanomaterial field, more experimental documentation is needed. To this end, we have carried out an *in situ* x-ray-diffraction study of nano-CeO<sub>2</sub> up to pressures of 38.6 GPa. We found that at room temperature the cubic fluorite phase of nano-CeO<sub>2</sub> undergoes a pressure-induced phase transformation at 22.3 GPa, which is remarkably lower than the pressure of 31 GPa occurring in the corresponding bulk CeO<sub>2</sub>. Another structure

phase was also observed in the recovered sample. These results are presented below.

### II. EXPERIMENTS

The sample used here was commercial nanosized CeO<sub>2</sub>, with a particle size of 9–15 nm. It was identified as a cubic fluorite structure ( $Fm\bar{3}m, 225$ ) by using x-ray diffraction and Raman spectroscopy.<sup>7,14</sup> Because of the size effect, the x-ray-diffraction peaks are quite broad. Raman spectroscopy displays a peak at  $467\text{ cm}^{-1}$ , which is a little higher than the peak at  $465\text{ cm}^{-1}$  observed in the bulk CeO<sub>2</sub>. This peak can be assigned to the triply degenerate first-order Raman-active peak ( $F_{2g}$ ) of the cubic fluorite structure CeO<sub>2</sub>.<sup>7,15</sup>

Diamond with a 400- $\mu\text{m}$  culet was used in a gasket diamond-anvil cell. The gasket consisted of a hardened spring steel 400- $\mu\text{m}$  thick, pre-indented to 65  $\mu\text{m}$ . A 150- $\mu\text{m}$  diameter hole was packed with CeO<sub>2</sub> powder mixed with a fractional amount of platinum powder. Pressure was checked with the well-known equation of state (EOS) of platinum (Pt). Energy dispersive x-ray-diffraction spectra were collected with a fixed  $2\theta (=11^\circ)$  on the bending magnet beam line at the Cornell High Energy Synchrotron Source (CHESS), Cornell University. The energy calibration was done by the well-known radiation source (<sup>55</sup>Fe and <sup>133</sup>Ba). The angle calibration was done by using six peaks of the standard Au powder.

### III. RESULTS AND DISCUSSION

Figure 1 shows x-ray spectra of nano-CeO<sub>2</sub> up to pressures of 38.6 GPa in this study. The unit-cell parameters are calculated from the positions of the x-ray-diffraction peaks of the starting sample at one atmosphere pressure, which show a pure cubic fluorite phase with  $a_0 = 5.416 \pm 0.012\text{ \AA}$  in agreement with the powder-diffraction value of  $a_0 = 5.41134(12)\text{ \AA}$  for the bulk CeO<sub>2</sub>.<sup>14</sup> With increasing pressure, new peaks of the high-pressure phase started to occur at a pressure of 22.3 GPa, which is significantly lower than the

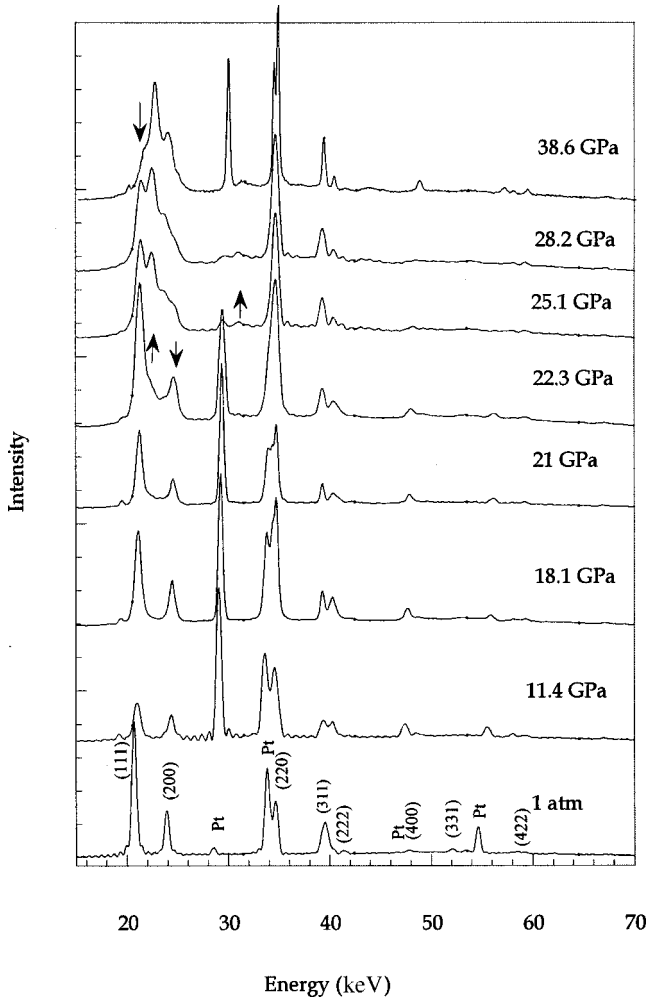


FIG. 1. X-ray diffractions of nano-CeO<sub>2</sub> up to pressures of 38.6 GPa. The downward arrow ↓ represents the disappearance of main peaks belonging to the starting phase of CeO<sub>2</sub>, and the upward arrow ↑ represents the appearance of some peaks of the high-pressure CeO<sub>2</sub> phase.

phase-transition pressure of 31 GPa occurring in the corresponding bulk CeO<sub>2</sub>.<sup>7,8</sup> Complete phase transformation to the high-pressure phase did not occur until a pressure as high as 38.6 GPa. This indicates that the phase transformation is quite sluggish and much slower than that taking place in the bulk material. It is suggested that a high-energy hindrance might be a factor that prevents the rapid formation of a high-pressure phase in nano-CeO<sub>2</sub>.

The high-pressure phase of CeO<sub>2</sub> can be effectively indexed to an orthorhombic cell with  $a_0 = 5.641(2)$ ,  $b_0 = 6.647(5)$ ,  $c_0 = 3.481(4)$  Å,  $V_0 = 130.53(8)$  Å<sup>3</sup> and four units of CeO<sub>2</sub> per unit cell at a pressure of 38.6 GPa. The bulk modulus was calculated to be 326(9) GPa, which is a little higher than 304 GPa found in the bulk CeO<sub>2</sub> by Duclos *et al.*<sup>8</sup> The unit-cell volume was extrapolated to ambient conditions and is 9.4% denser than the cubic fluorite. Upon release of pressure, the high-pressure orthorhombic phase becomes unstable and transforms to a different structure at a pressure of 4.0 GPa with the appearance of a few peaks that cannot be refined in both the cubic fluorite and the ortho-

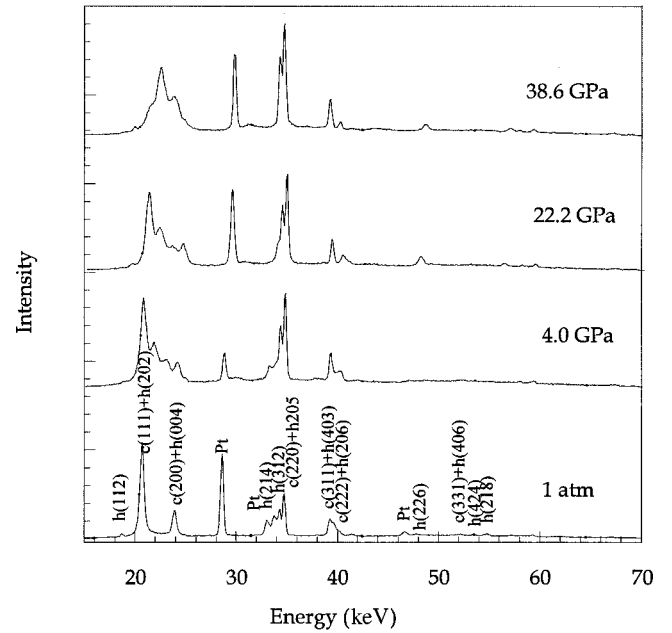


FIG. 2. X-ray diffractions of nano-CeO<sub>2</sub> with decompression to ambient conditions. The peaks at one atmosphere are marked with *c* and *h*, which represent the cubic fluorite phase and the hexagonal phase, respectively. The volume ratio of two phases is difficult to determine based only on the coexisting peaks.

rhombic structures. This recovered phase then remains stable to ambient conditions (Fig. 2). This is significantly different from the recovered phase in the bulk material, which has a cubic fluorite structure. The phase obtained can be well fitted to a hexagonal structure with  $a_0 = 8.368(11)$ ,  $c_0 = 10.693(15)$  Å,  $V_0 = 648.43(27)$  Å<sup>3</sup> (Table I), which is 2% less dense than the cubic fluorite phase at one atmosphere pressure due to a little distortion from the cubic structure.

Figure 3 shows the EOS data of nano-CeO<sub>2</sub> to pressures of 38.6 GPa. A fit to the Birch-Murnaghan EOS of the cubic

TABLE I. Observed and calculated *d* spacings of CeO<sub>2</sub> with the hexagonal structure at ambient conditions, which are recovered from high pressures. The unit-cell parameters are  $a_0 = 8.368(11)$ ,  $c_0 = 10.693(15)$  Å  $Z = 16$ , with  $V_0 = 648.43(27)$  Å<sup>3</sup>.

hkl	$d_{\text{obs}}$ (Å)	$d_{\text{calc}}$ (Å)	$d_{\text{obs}} - d_{\text{calc}}$ (Å)
101	5.969	5.101	-0.028
112	3.459	3.295	0.165
202	3.125	2.999	0.126
004	2.706	2.673	0.033
214	1.917	1.913	0.004
312	1.888	1.881	0.007
205	1.862	1.842	0.020
403	1.633	1.615	0.018
206	1.647	1.599	0.048
226	1.352	1.357	-0.005
406	1.241	1.270	-0.029
424	1.211	1.218	-0.007
218	1.184	1.201	-0.017

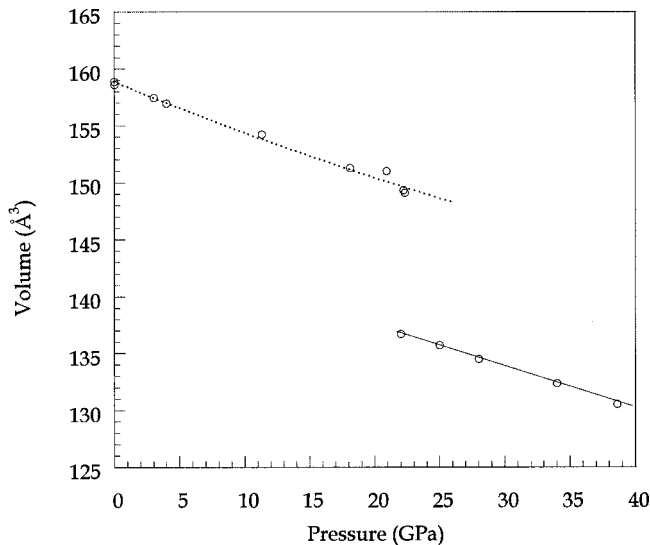


FIG. 3. The room-temperature equation-of-state data for nano- $\text{CeO}_2$ . The dotted curves are the Birch-Murnaghan equation-of-state fits for the cubic fluorite phase with  $B_0 = 328 \pm 12$  GPa,  $B' = 4$ . The high-pressure orthorhombic phase has  $B_0 = 326 \pm 9$  GPa,  $B' = 4$ . The density change extrapolated back to one atmosphere pressure is 9.4% between two phases.

fluorite phase gives the bulk modulus  $B_0 = 328 \pm 12$  GPa, when the bulk modulus pressure derivative is constrained to  $B' = 4.0$ . This is significantly higher than that of the corresponding bulk  $\text{CeO}_2$  with  $B_0 = 230$  GPa.<sup>8</sup> This indicates that the reduction of particle size significantly increases the bulk modulus.

Previous studies on nanosized materials indicate that the decrease of particle size leads to a large elevation of phase-transition pressure and of bulk modulus in nanomaterials, including sulfides and oxides, as compared to the bulk materials.<sup>9–13</sup> Recent studies on  $\gamma\text{-Fe}_2\text{O}_3$  and rutile ( $\text{TiO}_2$ ) show that the decrease of particle size results in a significant reduction of the phase-transition pressure in the pressure-induced solid-solid phase transformations.<sup>10,12</sup> The elevation of transition pressure in the pressure-induced solid-solid phase transformation has been explained by a higher surface energy between the phases involved in nanosized materials compared to the bulk materials. This is in agreement with the predictions of homogenous deformation theories.<sup>13</sup> Conversely, the reduction of transition pressure in another type of nanometric material has been interpreted by the large collapse in volume upon phase transformation due to the formation of the high-density high-pressure phase.<sup>10</sup> Our results obtained strongly support the existence of the transition-

pressure reduction in nanomaterials. So far, in addition to  $\text{CeO}_2$ , only two of the above-mentioned nanomaterials including  $\gamma\text{-Fe}_2\text{O}_3$  and rutile ( $\text{TiO}_2$ ) have been reported in the literature.<sup>10,12</sup> It is surprising that the corresponding high-pressure phases are unstable on release of pressure or upon increase of temperature. The nanosized rutile ( $\text{TiO}_2$ ) transforms to the  $\alpha\text{-PbO}_2$  phase at a lower pressure with the reduction of particle size, but with increasing temperature, the  $\alpha\text{-PbO}_2$  phase incorporates into the original rutile phase.<sup>12</sup> Even though the nanosized  $\gamma\text{-Fe}_2\text{O}_3$  was mostly fitted to the hexagonal structure at high pressures in the literature,<sup>10</sup> it is actually more reasonable to be substituted by a rhombohedral structure at high pressure due to a pressure-induced distortion. Upon release of pressure, it is recovered with the hexagonal phase. The above observations imply that the large volume collapse and the existence of an unstable high-pressure phase may lead to the reduction of transition pressure in nanomaterials compared to the corresponding bulk materials.

#### IV. CONCLUSION

This study has described the high-pressure room-temperature behavior of the nanosized  $\text{CeO}_2$ . The bulk modulus of the cubic fluorite structure nano- $\text{CeO}_2$  is  $328 \pm 12$  GPa with an assumption of a pressure derivative of 4.0. This clearly indicates that the reduction of particle size leads to a significant elevation of the bulk modulus of  $\text{CeO}_2$ . The nano- $\text{CeO}_2$  starts to transform on loading to an orthorhombic structure of space group  $Pnam$  at 22.3 GPa, which is significantly lower than the transition pressure of 31 GPa for the corresponding bulk  $\text{CeO}_2$ . Moreover, the reduction of particle size results in a quite sluggish dynamic process in the pressure-induced phase transformation of nano- $\text{CeO}_2$ . Upon release of pressure, the high-pressure orthorhombic phase becomes unstable. At a pressure of 4.0 GPa, it transforms to the hexagonal structure and then remains stable to ambient conditions. Thus, it may be suggested that a large volume collapse and the existence of an unstable high-pressure phase lead to a reduction of the transition pressure in nano- $\text{CeO}_2$ .

#### ACKNOWLEDGMENTS

We wish to thank the Division of Sponsored Research at Florida International University, which made this research possible. Also we acknowledge the assistance of the entire CHESS staff, leading to the successful collection of high-pressure x-ray-diffraction data at CHESS, Cornell University. Finally, special thanks go to Debby Arnold for her kind editorial assistance.

\*Email address: zwang04@fiu.edu

<sup>1</sup>G. A. Kourouklis and E. Anastassakis, Phys. Rev. B **34**, 1233 (1986).

<sup>2</sup>L. G. Liu, Earth Planet. Sci. Lett. **49**, 166 (1980).

<sup>3</sup>L. G. Liu, J. Phys. Chem. Solids **4**, 331 (1980).

<sup>4</sup>D. D. Schmidt and K. Vedam, J. Phys. Chem. Solids **27**, 1563 (1966).

<sup>5</sup>G. A. Samara, Phys. Rev. B **2**, 4194 (1970).

<sup>6</sup>J. R. Kessler, E. Monberg, and M. Nicol, J. Chem. Phys. **60**, 5057 (1976).

<sup>7</sup>G. A. Kourouklis, A. Jayaraman, and G. P. Espinosa, Phys. Rev. B **37**, 4250 (1988).

<sup>8</sup>S. J. Duclos, Y. K. Vohra, A. L. Ruoff, A. Jayaraman, and G. P. Espinosa, Phys. Rev. B **38**, 7755 (1988).

<sup>9</sup>J. Z. Jiang, J. S. Olsen, L. Gerward, D. Frost, D. Rubie, and J. Peyronneau, Europhys. Lett. **50**, 48 (2000).

- <sup>10</sup>J. Z. Jiang, J. S. Olsen, L. Gerward, and S. Morup, *Europhys. Lett.* **44**, 620 (1998).
- <sup>11</sup>S. B. Qadri, J. Yang, B. R. Ratna, E. F. Skelton, and J. Z. Hu, *Appl. Phys. Lett.* **69**, 2205 (1996).
- <sup>12</sup>J. S. Olsen, L. Gerward, and J. Z. Jiang, *J. Phys. Chem. Solids* **60**, 229 (1999).
- <sup>13</sup>S. H. Tolbert and A. P. Alivisatos, *Science* **265**, 373 (1994).
- <sup>14</sup>Powder-diffraction file: PDF No. 34-397 with  $a_0 = 5.411\ 34(12)\ \text{\AA}$ .
- <sup>15</sup>Z. W. Wang and S. K. Saxena, *Solid State Commun.* **118**, 75 (2001).